ACCURACY ANALYSIS OF DEMs GENERATED FROM UAS IMAGERY AND LARGE FORMAT DIGITAL CAMERAS

ricardopassini2012@outlook.com
dday@ksurveys.com[(a)]
wweaver@kasurveys.com[(a)]
jacobsen@ipi.uni-hannover.de[(b)]

(a) Keystone Aerial Surveys, Inc; (b) Leibniz University Hannover

KEY WORDS: UAS, aerial photography, AAT, bundle block adjustment, self-calibration, point cloud, DSM, DTM, accuracy

ABSTRACT:

This study has purpose of testing the achievable accuracy (absolute and relative) of DEMs generated by large format high resolution digital images and those generated by imagery taken by drone cameras. To this end a test area consists 0.043 Km2 (10.6 ACRES) of farm land that was flown initially with the UltraCam Falcon Prime (UCFp) and almost simultaneously with the Sony a7R with 35mm lens and the Cannon EOS Rebel SL1 with 20mm focal length mounted in a Steadi-Drone Mavrik X8 Octoquad UAS and the Altavian F6500 fixed wing UAS respectively. The imagery from the drones were AAT and bundle block adjusted with self-calibration. The same GCPs for the orientation of the UCFp imagery was used. Subsequently, three point clouds were derived, namely: from the UCFp and from the imagery taken by each camera drone. The drone point clouds were corrected by the effect of the systematic error of each corresponding camera. Accuracy testing were carried out individually to each generated cloud of points. The final accuracy test was performed comparing the three generated DEMs. As reference for comparison the UCFp generated height information was used. An intensive analysis was derived including complete statistical analysis.

1. INTRODUCTION

UAVs offer a considerate option while directing at large scale aerial mapping for areas of limited extent. Although flight designs are very flexible, particularly if rotary systems are used, many UAV projects are still taken by strip-wise flight arrangements. Thus, standard photogrammetric block geometry is available as input for traditional photogrammetric data acquisition. For such sceneries only minor alterations are required to calculate and reconstruct objects from the collected imagery by of-the-shelf commercial software products. By these means tasks like Automatic Aerial Triangulation (AAT), the generation of Digital Elevation Models and Orthoimages can be solved efficiently. In addition to such standard products, the application of dense image matching for the generation of high quality 3D point clouds has become a task of growing importance. Based on methods like the Semi-Global Matching (SGM) the stereo method of Hirsch-Muller (2008), surface reconstruction is feasible with a resolution at the ground sampling distance of the captured imagery. The potential of SGM for image data from digital airborne camera systems is for example presented in (Haala & Rothermel, 2012). In these investigations, matching accuracies better than 0.2 pixels permitted the generation dense 3D points even for areas of very inadequate texture. The available redundancy also allows for an efficient elimination of erroneous matches and resulted in a considerable reliability of the 3D points at vertical accuracies well below the sub-pixel level. Nevertheless, the mentioned test were conducted using digital metric cameras that provide airborne images with excellent dynamic range as well as signal-to-noise ratio that are highly beneficial for automatic image matching. A different state of the art is observed in the UAVs platforms that are frequently equipped with COTS cameras. Their small pixel size results in limited radiometric quality. Moreover the use of inexpensive optics and material of the camera body reduces considerably the stability of the image geometry. On the other hand, the UAV images should be collected at a high overlap due to their low cruising speed. Hence, the photogrammetric processing of UAVs images can potentially benefit from the resulting redundancy which would still allow the generation of high quality3D points cloud from dense multiple image matching.

The presented study has the purpose to test the achievable accuracy of DEMs derived from images obtained from UAVs as compared with DEMs obtained from digital high resolution large format aerial photography. With this purpose a farming area of about 10.6 acres was flown with an UltraCam Falcon Prime and almost simultaneously with

a. Steady-Drone Mavrik X8 Octoquad UAS equipped with a Sony a7R with 35mm lens (from now on called Sony) with 7390 x 4912 pixels of 4.9 µm.
b. Altavian F6500 fixed wing UAS equipped with a Canon EOS Rebel SL1 camera with a 20mm lens (from now on called Canon) with 5288 x 3506 pixels of 4.3 µm.

Both flights were carried out at 400 feet above ground (AGL), meaning that the mean image scales were 1:3,483 and 1:6,096 corresponding to 17 mm and 26 mm ground sampling distance (GSD) respectively.

2. DATA ACQUISITION

In this study two Digital Elevation Models (DEMs) using the above described sensors have been analyzed. With this purpose an almost flat area of about 10 acres in a farming area of Perkasie (PA), was flown by Keystone Aerial surveys (KAS) using its Ultra*C*am Falcon Prime of 100 mm focal length and 11310 x 17310 pixels of 6 µm pixel size corresponding to a GDS of 2 cm. The flight was done with 60 and 30% overlaps and the entire area was covered by 6 images arranged in two consecutive strips. A total of 15 targeted GCPs / Check Points were determined with a standard deviation of ~ 2 to 3 cm. Figures 1 shows a color coded DEM of the study area and Figure 2 the distribution of the GCPs / Check Points respectively.

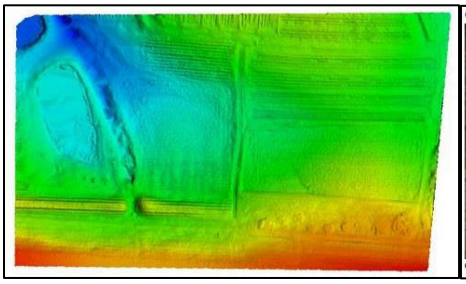

Figure 1. Color Coded DEM. UltraCam DEM

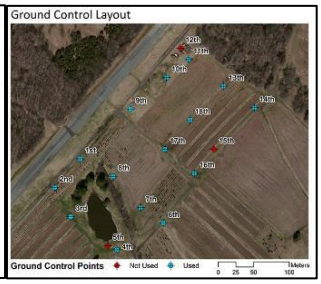

Figure 2. GCP Distribution

Almost at the same time the area was flown by the two mentioned UASs

To produce the desired DEMs the 3 sets of imagery had to be aerial triangulated and bundle block adjusted. Table 1 shows the flight parameters of the UASs carried out at 400 feet above ground (AGL).

Camera	Strips	Photos	Images/strip	Image Size(mm)	GCPs	Overlaps	# Tie Pts.	GDS	Platform (UAV)
Sony	4	72	18	35.034x23.3814	15	80%,60%	889,405	17 mm	Mavrik X8
Canon	7	201	29	22.7076x15.1384	15	80%,60%	2,221,043	26 mm	Altavian

Table 1. Geometric parameters of the UAS flights and initial AAT in Pix4D

Figure 3 shows the Sony image centers and flight pattern, the same is shown in figure 4 with respect to the Canon and figure 5 displays the Canon image footprints. Figure 6 shows the image foot prints of the Ultra*C*am Falcon Prime.

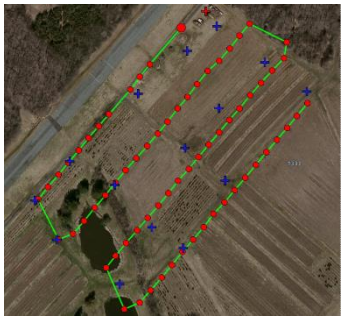

Figure 3. Sony image centers and flight pattern

Figure 4. Canon image centers and flight pattern

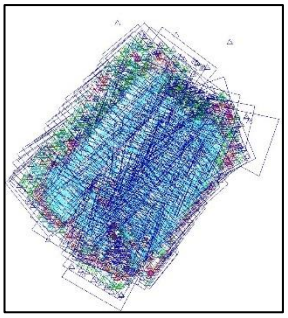

Figure 5. Canon image footprints

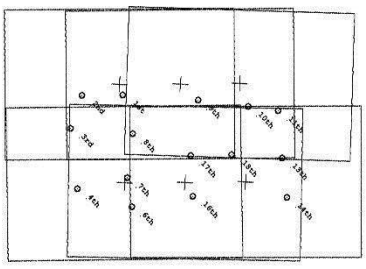

Figure 6. UltraCam Falcon prime Image footprints and location of targeted GCPs

All flown blocks firstly were aerial triangulated. For the automatic extraction of tie/pass points on the UASs flights the software Pix4D was used and for the Ultra*C*am Falcon Prime the AT module of Inpho. Simultaneous Least Squares Bundle Block Adjustment was done in all cases using the Leibniz University Hannover software BLUH. The results regarding the Ultra*C*am Falcon prime are shown in table 2 below:

	No self-calibration				Additional parameters 1 – 12				Parameters 1 – 12 + camera specific			
# GCPs	σ_o (μm)	RSX (m)	RSY (m)	RSZ (m)	σ_o (μm)	RSX (m)	RSY (m)	RSZ (m)	σ_o (μm)	RSX (m)	RSY (m)	RSZ (m)
15	0.96	0.01	0.01	0.035	0.92	0.01	0.01	0.031	0.89	0.009	0.009	0.029

Table 2. Results of Bundle Block Adjustment of the UltraCam Falcon Prime.

From the table it is easy to see the presence (although very small) of systematic errors especially in the Z-Component that are removed/minimized there effects by self-calibration. Figure 7 shows the systematic deformation pattern of the Ultra*C*am Falcon Prime (scale of the drawing has been exaggerated to show the pattern, but the deformation is clear) and Figure 8 the residual systematic errors after bundle block adjustment using standard self-calibration plus camera specific additional parameters:

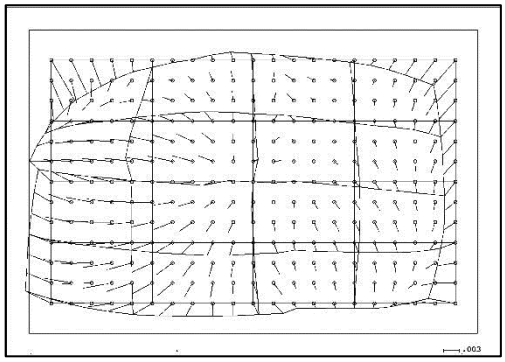

Figure 7. Systematic deformation pattern

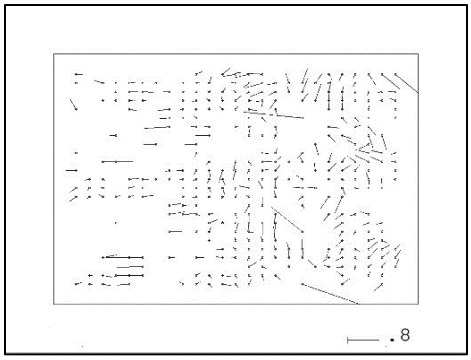

Figure 8. Residuals systematic errors after self-calibration

Figure 7 shows clearly systematic radial symmetric distortion and in the corners of another type. Figure 8 shows the residual systematic errors after standard and camera specific self-calibration. Although the majority much smaller than 0.8 μm. Some of them up to ~ 1.5 to 2.0 μm

They might be responsible of some model deformation on the product to be derived (Basic DEM)

Both cameras used on the UASs flights are COTS instruments and as such they do not have metric characteristics. This produced large impacts (image deformation) on the images that are acquired through them. Their lack of metrics characteristic are portrayed through systematic errors included in those images and consequently on any Photogrammetric product derived from them. As the aim is to statistically compare DEMs derived from these UASs-non-metric cameras with the Ultra*C*am derived DEM, the starting point should be to analyze the accuracy statistics of the corresponding aerial triangulation adjustment, including self-calibration, for the elimination of deformations. With this purpose, once again the Leibniz University Hannover program package BLUH was used. Results are shown in Table 3:

	No self-calibration				Additional parameters 1 – 12				Additional parameters 1 – 12 + 81 – 88			
Camera	σ_o (μm)	RSX (cm)	RSY (cm)	RSZ (cm)	σ_o (μm)	RSX (cm)	RSY (cm)	RSZ (cm)	σ_o (μm)	RSX (cm)	RSY (cm)	RSZ (cm)
Sony	4.1	1.5	1.0	8.0	3.8	1.1	1.0	3.9	3.7	1.0	0.9	3.2
Canon	4.5	5.3	5.1	11.1	3.9	1.5	2.3	7.3	3.8	1.2	2.14	5.1

Table 3. Results of the bundle block adjustment with and without self-calibration

Although the above results are very encouraging they show residual block deformation that is noticeable in the Z-component in spite of the use of standard additional parameters (1 through 12) and those corresponding to the small cameras (81 through 88). These remove the systematic effects on the image corners and respect the lack of planarity of the chips over the focal plane

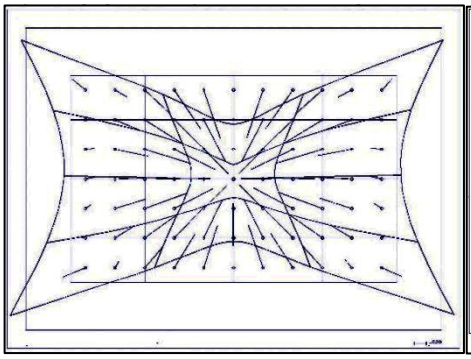

Figure 9. Systematic errors pattern, Canon.

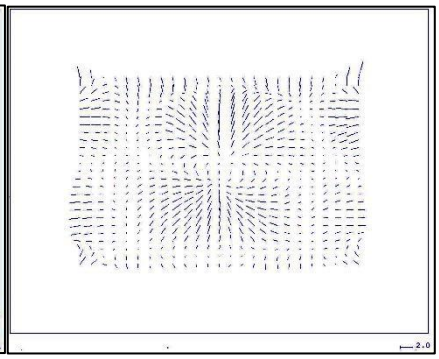

Figure 10. Residuals systematic errors, Canon

Figure 9 clearly shows the strong component of the radial symmetric distortion with different magnitudes and directions of the Canon camera. These distortions are not entirely removed by self-calibration as it is shown in Figure 10. Figure 11 shows a different systematic error pattern for the Sony Camera and the residual systematic errors (after self-calibration) that are different in magnitude and direction are shown in Figure 12

The not respected systematic image distortions will deform any 3D model based on those images. In particular, the intention to derive a DEM using the cameras mounted on the UAS, with the full understanding of the geometry of the images and systematic

errors. These errors can be determined and respected in the block adjustment through self-calibration with additional parameters. Nevertheless, the systematic deformations remain in the images after any aerial triangulation procedure that includes self-calibration. Most digital photogrammetric software producing DEMs are not able to respect systematic image errors, causing the resultant DEMs to be influenced by model deformations caused by these systematic image errors. Part of the software package BLUH, DEMCOR can correct DEMs influenced by model deformations and was applied to the DEMs generated by the UAS imagery on in this study.

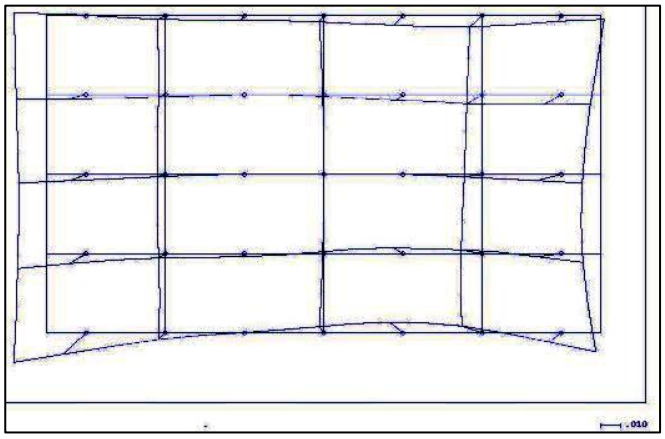

Figure 11. Systematic error pattern. Sony

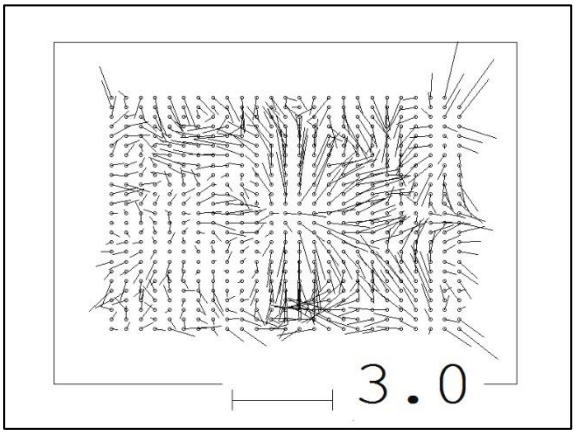

Figure 12 Remaining systematic errors. Sony

The UltraCam generated DEM (From now on to be called Basic DEM) consisted of a 50 x 50 cm grid covering the research area. Using the GCPs as check points the LiDAR DEM was Quality Controlled generating the following results (in meters):

Average DZ -0.031 m
Minimum DZ -0.263 m
Maximum DZ +0.082 m
Root mean square (RMSZ) 0.088 m

3. - DEM ANALYSIS

The Canon and the Sony DEMs, once corrected by the remaining systematic errors through program DEMCOR, were statistically compared with the Basic DEM. To accomplish this, DEMANAL (also part of the BLUH package) was used to create a statistical comparison (nearly 350,000 points for analysis from each COTS originated DEM) producing the following results in centimeters:

Statistics diff of DEMs	Camera on UAV	RMSZ	BIAS	SZ no bias	RMSZ Eucl	Eucl RMS no bias	NMAD
	Canon	8.3	-1.8	8.1	8.1	7.9	4.7
	Sony	12.5	-7.9	9.7	12.2	9.4	6.3

Table 4.Simple statistics between DEMs. NMAD: Normalized Mean Absolute Deviation. Eucl: Euclidean Distance

It is known from statistics that if the discrepancies are normally distributed the Standard Deviation (SZ) (based on square sums) and Normalized Mean Absolute Deviation (NMAD) (based on median of absolute differences) should be identical. Table 4 clearly shows that they are not. This difference can easily be attributed to the effect of the higher number of large discrepancies as corresponding to normal distribution which may cause by not respected remaining systematic errors.

The area used for the study has small undulations, nevertheless it is worthwhile to derive the RMSEz (regular and according to Euclidean distances) as a function of the slope. These are depicted in table 5 in meters

Type	RMSEz of DEM differences as a function of the slope of the terrain					
	UCFp to Sony			UCFp to Canon		
		SZmin	SZmax		SZmin	SZmax
Regular RMSEz	SZ = 0.195 + 0.430 * tan(slope)	0.195	0.201	SZ = 0.137 + 0 .463 * tan(slope)	0.137	0.143
Euclidean RMSEz	SZ = 0.216 + 0.094* tan(slope)	0.216	0.217	SZ Eucl = 0.169 +0.118*tan(slope)	0.169	0.171

Table 5. RMSEz of the DEMs differences as a function of the slopes in meters. Max Slope 0.75

Once again (for the terrain of the study) the slope plays almost no effect on the Standard deviation of the differences between the DEMs under study (See SZmin and SZmax). Nevertheless, smaller values are observed, especially in those related to the

Euclidean distances. This distance is taken from the point of the DEM under study measured perpendicularly to the reference DEM, in this case the UCFp generated DEM. Hence the smaller computed values are justified.

Type	RMSEz of DEM differences as a function of the slope of the terrain (no Syst. Errors)					
	UCFp to Sony			UCFp to Canon		
		SZmin	SZmax		SZmin	SZmax
Regular RMSEz	SZ = 0.172 + 0.332 * tan(slope)	0.172	0.176(12%)	SZ = 0.134 + 0 .402 * tan(slope)	0.134	0.139(2.8%)
Euclidean RMSEz	SZ = 0.156 + 0.105* tan(slope)	0.156	0.157(28%)	SZ Eucl = 0.158 +0.117*tan(slope)	0.158	0.160(6.4%)

Table 6. RMSEz of the DEMs differences (without systematic part) as a function of the slopes in meters. Max Slope 0.75

When systematic errors are removed, then the gain in accuracy in terms of SZ is visible. In the SZ max values are between 2.8% and 28%. One can also notice the higher gain corresponds to the difference Basic DEM – Sony DEM. See table 6 and compare Tables 5 and 6. This can be expected due to higher systematic errors and noise present in the Sony Images (See Table 4 and Figure 12)

In relation to the stochastic variable NMAD and its values for the difference of the DEMs in relation to the slope:
NMAD = 0.117 + 0.483 * tan (slope) NMAD min=0.117, NMAD max = 0.123 (UCFp – Sony)
NMAD = 0.020 + 0.603 * tan (slope) NMAD min=0.020, NMAD max = 0.028 (UCFp – Canon)

Once again (for the terrain of the study) the slope plays a non-significant role on the values of NMAD. Higher values are visible from the DEM difference UCFp – Sony. This mean that the larger systematic errors of the Sony images (See Table 4) are affecting the DEM derived from them. Smaller values are observable for the DEM difference UCFp – Canon. This can be justified by the lower magnitude of the systematic errors of the Canon camera (See Table4). Moreover, the flight is more stable and smooth due to the fixed wings. Hence there is almost no noise effect added to the residual systematic effects.

Another interesting aspect to be studied is the frequency distribution of DEM differences (DZ)

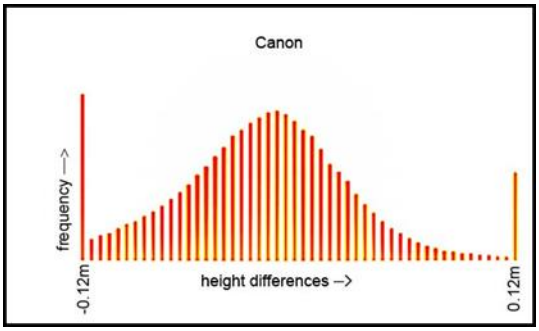

Figure 13. DZ Frequency distribution UCFp vs. Canon

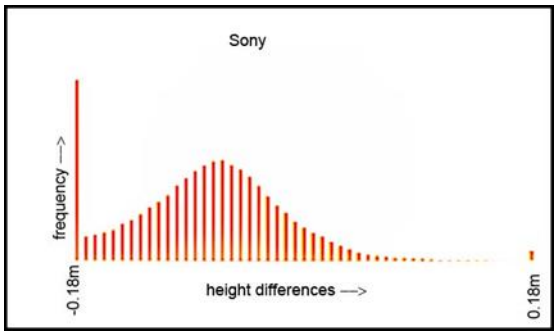

Figure 14. DZ Frequency distribution UCFp vs. Sony

Both frequency distribution appears to be Normally Distributed. Nevertheless, both have biases approximately -2 cm (UCFp-Canon) and -8 cm (UCFp-Sony). Moreover, both have gross errors in the DZ intervals of 12 and 18 cm. As shown also in Table 4 above, neither are symmetrical with respect to the DZ interval with higher frequency. This can be mainly attributed to the remaining systematic errors still present in the images, whereas the gross errors in the intervals of 12 and 18 cm can easily be attributed to errors in the clean-up of the vegetation (DSM to DTM). Although a similar pattern is seen in both frequency distribution functions, the difference between the UCFp and the Canon appears more uniform than the other. This can also be noticed in figures 15 and 16 that show the 2D color coded geographical representation of the DZ.

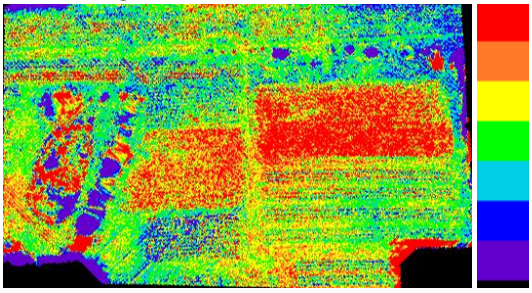

Figure 15. 2D Color coded representation of DZ in UCFp-Canon comparison

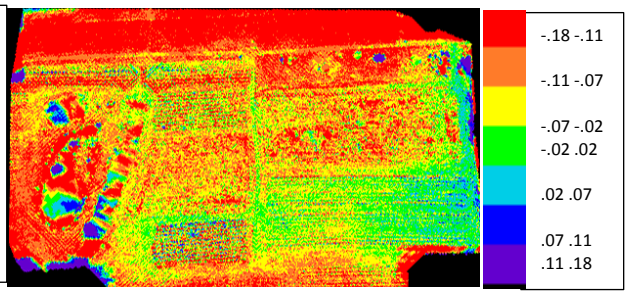

Figure 16. 2D Color coded representation of DZ in UCFp-Sony comparison

Figure 16 shows a large amount of DZs within the interval -18 to -11 cm that can be shown in the frequency distribution of the UCFp-Sony, whereas in the Figure 15 the green color predominates, that is for the interval -1 to 2 cm that can also be observed in the frequency distribution of the UCFp-Canon.
The general expectations is that:
There should be no systematic DEM differences between the DEM produced by one or another combination of platform/sensor once all possible corrections are applied, but it is important to mention the following facts:

a. Acquisition platforms have different characteristic affecting image quality.
b. Data acquisition systems have different resolving power and image quality.
c. The systematic errors introduced by each combination of platform/data acquisition system and their instrument to acquire ancillary information are different in nature and magnitude
d. The cameras under consideration here are made of different alloys, system of lenses, image electronic chips, etc. They have not been specifically produced for geospatial information collection. Being COTS products they are not designed for metric purposes.
e. The platforms (UAS) used during this research are of a totally different nature. One is a rotorcraft, while the other is a fixed wing. Hence the vibrations (which can be translated into systematic image errors) are completely different in nature and magnitude.
f. The UltraCam Falcon Prime was flown using an airplane prepared for the mission with minimal or absence of vibrations

In other words, it is mathematically impossible to remove the effects of all the sources of errors. Additionally, the Sony has 17mm GSD, while the Canon has 26mm GSD and the field of view for Canon is approximately 10% larger as for Sony. The larger field of view and larger GSD of Canon by simple theory should result in 38% larger standard deviation of height as for the Sony, but table 3 shows a 18% smaller SZ. It is also known that the slope of the terrain plays an important role in the derivation of the vertical accuracy. Unfortunately the chosen area for the research did not have significant geomorphological variation in terms of slope and aspect. The reference DEM is based on the metric camera UCFp with approximately 20mm GSD, being similar to the GSD taken by the small format COTS cameras. Of course the metric camera has a better geometric condition and the large format avoids a deformation of the generated DEM. Nevertheless, from the results of the investigation some valid conclusions can be drawn.

4. - CONCLUSSIONS

1. The accuracy in terms of Standard Deviation (σ_o) and RMSEz of the UltraCam Falcon Prime Aerial Triangulation were 0.89 µm and 3 cm exceeding all expectation. Notwithstanding the RMSEz of the derived (base) DEM computed based on the Targeted GCPs was in the order of 7 to 8 cm which is not far away from the accuracy of the DEMs based on the UAVs carried small format cameras compensating some disadvantages by the high number of images.
2. In relation to the results of the ATT performed with the COTS cameras installed in the respective drones, the results of such least squares adjustment shows:
    a. Quite different systematic deformation patterns, magnitude of errors and direction are apparent.
    b. The 12 standard additional parameters could remove majority of the effect of the distortion reducing the RMSEz of the bundle block adjustment over the GCPs from 8 cm to 4 cm for Sony and from 11cm to 7 cm for Canon. (See Table 3). Further systematic distortion effects were possible to be eliminated through the introduction of parameters 81 through 88 that takes into consideration the lens cone deformations towards the corners of the camera and the lack of flatness of the image chips over the focal plane. The accuracies in terms of RMSEz is reduced to 3.2 and 5.15 cm respectively for the Sony and Canon arrangement with the use of these parameters (See Table 3).
    c. As shown in Figures 10 and 12, there still limited amounts of remaining systematic errors after the self-calibration bundle block adjustment. To totally eliminate/minimize their impact in the adjusted EOs new functional models for self-calibration need to be derived.
    d. Nevertheless, by bundle block adjustment with self-calibration only the systematic image errors are determined. If they are not respected by a change of the geometry of the digital images for the determination of the height models they are causing some model deformations, also caused by the correlation of the systematic image errors to the image orientation.
    e. The NMAD (Normalized Mean Absolute Deviation) describes the frequency distribution of the height differences better as the standard deviation. Is a robust measure of the variability of a univariate sample (DZ) of quantitative data and less sensitive to the blunders as it is the standard deviation/RMSE, reported an accuracy increase by 43% (Canon system) and by nearly 50% (Sony system) with respect to both achieved RMSEz (see Table 3).
    f. Within the study area, regardless of the UAS/camera used, the slope of the terrain under study has almost no influence in the RMSEz of the differences between surface DEMs. This is in relation to the regular vertical differences or the Euclidean differences (see Table 5). If the systematic errors are removed, then the gain in accuracy can be considerable. For regular vertical differences 2.8% for the Canon to 12% for the Sony. Regarding

the Euclidean distances, 6.4% for the Canon to 28% for the Sony (compare Tables 4 and 5). This gain in accuracy is evident in the Sony imagery set with 17mm GSD while it is 26 mm for the Canon images set and as such the effects of the systematic errors are multiplied more. The same can be observed when NMAD is taken into consideration.

g. Both DZ frequency distribution functions are similar to a Normal Distribution Function (See Figures 13 and 14). They have approximately -1.5 and -7.5 centimeter biases for the sets Canon and Sony respectively. These are similar to the values reported in Table 4. Moreover, both distributions are not entirely symmetrical with the DZ interval with higher frequency. Thus, the canon set frequency distribution function has a kurtosis of 0.27 and a skewness of 0.28; whereas for the Sony set these values are 1.29 and 0.92 respectively. Both anomalies can be attributed to the remaining systematic errors in the COTS camera images. Moreover, the negative nature of the biases suggests that the majority of the homologous/corresponding points of the COTS imagery intersects in the space bellow the reference DEM surface. Another effect only attributed to the systematic errors.

h. The frequency distribution function of the univariate DZ and their 2D graphical representations (See Figures 15 and 16) show that those derived from the Canon set are more uniformly distributed than the Sony set or at least with smaller shift. The larger magnitude of DZ can be explained by the different ground sample distance. The majority of the DZ are included within the interval --0.10 and 0.05 m.

5. RECOMMENDATION

The majority of the applications where the use of a UAS with a COTS camera is economically justified the results being obtained during the orientation of the images as well in the modeling of the test area are sufficient for most applications. Only those applications requiring engineering grade accuracy demand the use of tools for self-calibration functions. In such case it is recommendable also to perform at least a laboratory calibration of the lens system prior to initiate the flight (see Figures 9 and 11). A field systems calibration it is preferable but this depends on the available time and resources.

6. REFERENCES

R. Passini, et al (2017): A Study on Accuracy on DEMs generated from UASs Imagery as Compared with latest generation LiDAR. In the Proceedings of the International LiDAR Mapping Forum 2017. Denver (CO), February 13 – 15, 2017. 5 pages

Jacobsen, K. (2016): Analysis and Correction of Systematic Height Model Errors. In: Int. Arch. Photogramm. Remote Sens. Spatial Inf. Sci. XLI-B1, pp. 333-339

R. Passini; K. Jacobsen; D. Day; S. Quillen (2013). A study on accuracy and fidelity of terrain reconstruction after filtering DSMs produced by aerial images and Lidar surveys. ASPRS National Convention, Baltimore, March 24-28, 2013. 6 pages

Büyüksalih, G.; Jacobsen, K. (2014): Comparison of Height Models from High Resolution Aerial Images and from LiDAR. 34th EARSeL Symposium, Warsaw, June 2014, 7 pages

Jacobsen, K. (2013): DEM Generation from High Resolution Satellite Imagery, PFG 2013 / 5, pp 483–493

Jacobsen, K.; Passini, R. (2010): Analysis of ASTER GDEM Elevation Models, In: IntArchPhRS vol. XXXVIII, part 1, Calgary, 2010, 6 pages

Passini, R.; Jacobsen, K. (2007): High Resolution SRTM Height Models: IntArchPhRS XXXVI. Band 1/W51. Hannover, 2007, 7 pages.

Jacobsen, K. (2006): SRTM Height Models. In: GeoConnexion International Magazine 5 (2006), Nr. 7, pages 20-21

Büyüksalih, G.;Kocak, G.;Oruc, M.;Akcin, H.;Jacobsen, K. (2004): Accuracy Analysis, DEM Generation and Validation using Russian TK-350 Stereo-Images. In: The Photogrammetric Record 19 (2004), Nr. 107, pages 200-218

Lohmann, P.;Jacobsen, K. (2004): Filterung segmentierter Oberflächenmodelle aus Laserscannerdaten. In: PFG (2004), Nr. 4, pages 279-287

Büyüksalih, G.;Kocak, G.;Jacobsen, K. (2004): Quality assessment of DEM derived from the SRTM X- and C-band Data: A Case Study for Rolling Topography and Dense Forest Cover: EARSeL- Workshop. Kairo, 2004, 6 pages.

Jacobsen K. (2001): New Developments in Digital Elevation Modelling, Geoinformatics, June 2001, pages.18-21

Jacobsen, K.;Lohmann, P. (2003): Segmented Filtering of Laserscanner DSMs., IntArchPhRS XXXIV, 3/W13, Dresden, 2003

Passini R.; Betzner D.; Jacobsen K. (2002): Filtering of Digital Elevation Models, ASPRS Annual Convention, Washington, 2002, 9 pages.